Heliyon 9 (2023) e21807

Contents lists available at ScienceDirect

Heliyon

journal homepage: www.cell.com/heliyon

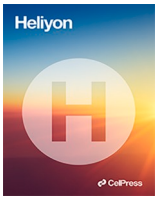

Stability of magnetohydrodynamics free convective micropolar thermal liquid movement over an exponentially extended curved surface

Aisha M. Alqahtani [a], Zeeshan [b], Waris Khan [c,*], Amina [d], Somayah Abdualziz Alhabeeb [e], Hamiden Abd El-Wahed Khalifa [f,g]

[a] Department of Mathematical Sciences, College of Science, Princess Nourah Bint Abdulrahman University, P. O. Box 84428, Riyadh, 11671, Saudi Arabia
[b] Department of Mathematics & Statistics Bacha Khan University, Charsadda, KP, 24420, Pakistan
[c] Department of Mathematics & Statistics, Hazara University, Mansehra, 12120, KP, Pakistan
[d] Department of Physics Bacha Khan University, Charsadda, KP, 24420, Pakistan
[e] Department of Mathematics, College of Science and Arts, Qassim University, Al-Mithnab, 51931, Saudi Arabia
[f] Department of Mathematics, College of Science and Arts, Qassim University, Al-Badaya, 51951, Saudi Arabia
[g] Department of Operations and Management Research, Faculty of Graduate Studies for Statistical Research, Cairo University, Giza, 12613, Egypt

ARTICLE INFO

Keywords:
bvp4c and ND-Solve
Micro polar thermal liquid
Nanomaterial
Nanofluidics
Heat source
Variable thermal conductivity
Exponentially extended curved surface

ABSTRACT

Micro polar fluids have a wide variety of applications in biomedical, manufacturing, and technical activities, such as nuclear structures, biosensors, electronic heating and cooling, etc. The aim of this study is to investigate the properties of heat transfer on a magnetohydrodynamic free convection movement of micro polar fluid over an exponentially stretchable curved surface. The flow is non-turbulent and steady. The effects of Joule heating, varying thermal conductivity, irregular heat reservoir, and non-linear radiation are anticipated. The modelled PDEs are converted to ODEs via transformation, and the integration problems are then addressed using ND-Solve method along with bvp4c package. It is observed that velocity is reduced and the micro rotation field is increased as the micro rotation parameter is increased. It is witnessed that the temperature of the fluid enhances as the Eckert number is augmented. The velocity is increasing function of the curvature parameter while the decreases with increasing magnetic factor. The distribution of temperature is improved by a rise in temperature-dependent thermal conductivity characteristic. It is investigated that as the values of temperature ratio, Prandtl number, and the Biot number are increased the temperature distribution is enhanced. For the stability of the numerical results, the mean square residue error (MSRE) and total mean square residue error (TMSRE) are computed. For the confirmation of the present analysis, a comparison is done with the published study and excellent settlement is found.

1. Introduction

Numerous studies have been done on fluid flow past stretched surfaces recently, but in the last ten years, various investigations has

* Corresponding author.
E-mail address: wariskhan758@yahoo.com (W. Khan).

https://doi.org/10.1016/j.heliyon.2023.e21807
Received 15 May 2023; Received in revised form 27 October 2023; Accepted 29 October 2023
Available online 4 November 2023

been carried out on micro polar fluid flow through solid surfaces due to the significance of this analysis for manufacturing and industrial applications. Micro polar liquids and heat transfer has been the subject of several articles and investigations. Recently, several publications have discussed the relevance of the effects of micro sized fluids in a variety of industries, including the glass industry, the military, nuclear reactors, solar energy and urine flow in the kidneys and bladder. The fluid dynamics of an extended stretched sheet and the works that may specify the properties of non-Newtonian liquids are important in several practical applications, including the manufacturing of paper, glass, metal, and rubber sheets. While studying the viscous liquid properties across an extended curved surface, it was concluded that the curvature component has a tendency to diminish the boundary layer thickness (BLT) [1]. The micro polar liquid boundary layer flow (BLF) over solid sheet having chemical response was investigated numerically. The homotopy analysis technique is used to deal with the changed equations [2]. In addition, the feature of viscoelastic stagnation point flow on an exponentially stretched sheet was also investigated [3]. In order to understand how an extended curved surface affects the porous medium structure, Saleh et al. [4] looked at the unsteady movement of shear thickening liquefied. Subjected to a solid surface, Naveed et al. [5] suggested coincident explanations to hydro-magnetic viscoelastic fluid. Currently, researchers [6,7] carried out computational analysis to unsteady Williamson liquid with heat transport movement along a curved sheet.

In addition to astrophysics, geology, the medical industry, and powered manufacturing, MHD study has substantial effects on these fields as well. The Lorentz force has essential uses in postures, forces, boundary layer regulator, and magneto hydrodynamic producers. Nadeem et al. [8] numerically investigated the hybrid nanofluid with heat analysis over porous stretched sheet with slip effect. When the Lorentz force is present, Alshomrani and Gul [9] demonstrated simultaneous solutions over a stretched cylinder for Al_2 O_3 and Cu-based water nanoliquids. Nadeem et al. [10] studied the hybrid nanofluid over a vertical elongated sheet of magnetized Casson fluid flow. Across a vertical surface in Carreau liquid, Anantha et al. [11,12] studied the drag force impact on the time-dependent bio convective mobility.

The effect of non-linear radiation on free convection movements exhibits an enormous attractiveness in space research as well as many manufacturing processes involving higher temperatures, for instance the metallic components cooling, paper plates production, petroleum pumps operation, and the electronic chips production. Nadeem et al. [13] theoretically investigated the non-Newtonian micro polar through an exponentially extending sheet along free stream phenomena. Sandeep et al. [14] investigated the characteristics of micro polar fluid heat transfer owing to surface elongating and discovered that as the radiation parameter rises, temperature does as well. The radiative heat flux effect on magnetohydrodynamic transport of viscoelastic liquid over a curved surface was also studied [15,16]. According to Zeeshan et al. [17], radiation and drag force affect how ferrofluid flows across a stretched sheet. The coupled equations are solved using the RK4 procedure. Anantha Kumar et al. [18] addressed a numerical analysis on the magnetohydrodynamic obliquely flow of micro polar fluid across a stretched sheet under the influence of non-linear radiation.

The phenomenon of irregular heat source/sink has a wide variety of uses in medical, bio-sciences, and several engineering events including radiating dampers, the aim of bearing insertion, and crude oil recovery. With variable heat source/sink, the heat mass transmission characteristics of non-Newtonian fluids have also been discussed in detail [19]. A first order chemical reactions impact on the MHD of a micro polar fluid across curved surface with radiation has been explored by Hayat et al. in their study [20]. The detail of significant used of non-Newtonian fluid over a stretched surface are given in Refs. [21,22]. Nadeem et al. [23] explored the heat mass transmission of micropolar fluid using Casson nanofluid passed through a vertical stretchable riga sheet. Ramzan et al. [24] explored te MHD effect on micro polar fluid over stretched surface. It was found that the heat has direct relation to Eckert and Biot number.

The physical features of the ambient fluid are taken into consideration in all the aforementioned articles, however different real-world scenarios require for physical features with diverse characteristics. One of these characteristics, which are extremely linear with temperature, is temperature-dependent thermal conductivity. Khan and Rafaqat [25] investigated the thermal magnetized compressible Jeffrey fluid. Abel and Mahesh [26] added radiation and regular heat reservoir to his study. In the occurrence of thermal conductivity, the magnetized viscoelastic fluid was studied on a stretched surface. Khan et al. [27] examined the behaviour of magnetized micropolar fluid passed through a curved stretchable sheet with modified Fourier law. The study of varied characteristics of magnetized non-Newtonian fluid flow across a stretched surface suggested that changing thermal conductivity increased the fluid temperature [28]. In the presence of thermal influence, Anantha et al. [29] examined the effects of varying temperature and viscosity upon magnetized non-Newtonian flow across a melted surface. Investigations were conducted into how the Biot value affected the magnetized movement of a viscous fluid across the exponentially expanding surface having variable fluid properties as well as a heat source/sink. It was determined that a thermal conductivity characteristic slow down the pace at which heat moves [30]. Metwally et al. [31] investigated the Sutterby fluid with radiation effect over a curved sheet. A theoretical research on the passage of a Newtonian fluid through a solid surface in magnetohydrodynamic bio-convective flow was described by Makinde and Animasaun [32]. The impression of heat flux on magnetohydrodynamic fluid flow via a stretched sheet using novel heat flux model was also studied [33].

Therefore, inspired by the abovementioned research, we attempted to investigate the free convection BLF across an exponentially expanding curved surface while taking into account changing thermal conductivity, nonlinear Rossland model, irregular heat source/sink, and Joule heating system. The theoretic model is deliberated for the suggested investigation, and after utilizing the right suitable transformations then computed numerically through ND-Solve approach along with BVPh2. The novel part of this study is to investigate the free convection boundary layer flow across an exponentially expanding curved surface in the presence of thermal conductivity, and irregular heat source/sink, which has not yet investigated. So, in limiting case the paper is compared with the published one. A graphical representation is utilized to study the inspirations of different controlling non-dimensional factors such as temperature, velocity and the micro rotation profiles. For the stability of the numerical results, the MSRE and TMSRE are computed. For the confirmation of the present analysis, a comparison is done with the issued study and decent settlement is found.

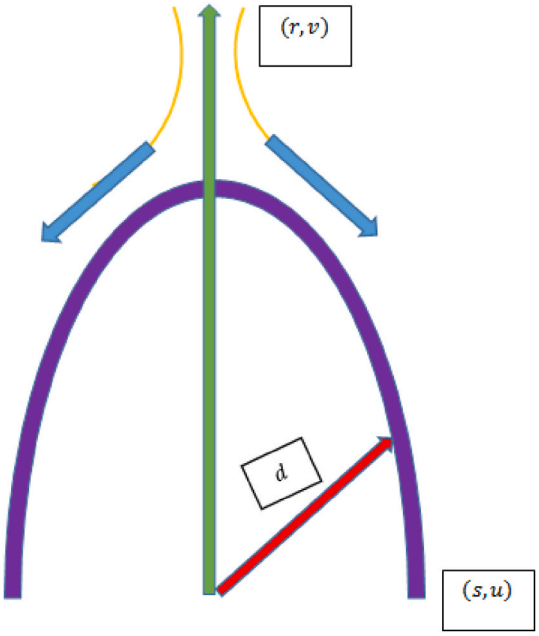

Fig. 1. Fluid geometry.

2. Mathematical modelling

Assume the flow of an incompressible micro polar, electrically conducting liquid across curved surface that is exponentially extending in a two-dimensional (2D) boundary layer with nonlinear heat radiation. It is anticipated that the movement is laminar, time-independent, magnetic Reynolds number and Ohmic heating are low, Joule heating, varying thermal conductivity, heat source/sink, and convective boundary are taken in the fluid flow problem. Suppose that the coordinate system is (r,s), with the r-axis being orthogonal to the direction of flow and the s-axis being considered in that direction. Let d represent the circle's radius. The surface is stretched with a velocity of $u_w(s) = A_1 e^{\frac{s}{L}}$ along the surface direction ($A_1, L > 0$) with an initial stretching rate A and reference length L. As publicized in Fig. 1, the magnetic field is constant and distributed in the radial direction.

The flow equations will be based on the above stated assumptions [3,15].

$$\frac{\partial}{\partial r}((r+d)v) + d\frac{\partial u}{\partial s} = 0, \tag{1}$$

$$\frac{\partial p}{\partial r} = \frac{\rho}{r+d}u^2 \tag{2}$$

$$\rho(v\frac{\partial u}{\partial r} + \frac{d}{(r+d)}u\frac{\partial u}{\partial s} + \frac{uv}{(r+d)}) = \frac{-d}{(r+d)}\frac{\partial p}{\partial s} - \kappa\frac{\partial N}{\partial r} - \sigma B_0^2 u + (\mu+\kappa)\left(\frac{\partial^2 u}{\partial r^2} + \frac{1}{(r+d)}\frac{\partial u}{\partial r} - \frac{u}{(r+d)^2}\right) \tag{3}$$

$$\rho j(v\frac{\partial N}{\partial r} + \frac{d}{(r+d)}u\frac{\partial N}{\partial s}) = \Gamma\left(\frac{\partial^2 N}{\partial^2 r} + \frac{1}{(r+d)}\frac{\partial N}{\partial r}\right) - \kappa\left(2N + \frac{\partial u}{\partial r} + \frac{u}{(r+d)}\right), \tag{4}$$

$$\rho C_p(v\frac{\partial T}{\partial r} + \frac{du}{(r+d)}u\frac{\partial T}{\partial s}) = \frac{1}{(r+d)}\left(\frac{\partial}{\partial r}((r+d)k(T)\frac{\partial T}{\partial r}\right) - \frac{\partial}{\partial r}((r+d)q_f)) - \sigma \tag{5}$$

In the directions (s,r), the velocity components are represented by (u,v). In addition, P is pressure (dimensional), η is viscosity (dynamic), ρ is density, C_p is heat capacitance, σ is electrical conductivity, $k(T)$ is temperature dependent thermal conductivity, T is fluid temperature, Γ is spin gradient viscosity, κ is vortex viscosity, q_f is radiated heat flux, and N is the micro-rotation (dimensional).

Let us now consider Γ and $k(T)$ [3].

$$\Gamma = \left(\mu + \frac{\kappa}{2}\right)j = \mu j\left(1 + \frac{\alpha_1}{2}\right)$$

$$k(T) = \kappa_\infty\left(1 + \varepsilon\left(\frac{T - T_\infty}{T_w - T_\infty}\right)\right) = \kappa_\infty(1 + \varepsilon\theta(\eta)) \tag{6}$$

Here, $\left(j=\frac{2L\nu}{A_1 e^{\frac{s}{L}}}\right)$ is micro-inertia, ε is the variable thermal conductivity parameter, k_∞ is the ambient fluid thermal conductivity, and α_1 is the micro polar parameter.

To investigate heat transfer performance in Eqn. (5), q_f is used, and it is defined as

$$q_f=\frac{-4\sigma^*}{3k^*}\frac{\partial T^4}{\partial r}=\frac{-16\sigma^*}{3k^*}T^3\frac{\partial T}{\partial}r, \tag{7}$$

The term "non-uniform heat source/sink" is added to equation (5) by the notation q^* and is given by

$$q^{'''}=k(T)u_m\frac{(s)}{2L\upsilon}(\mathrm{A1}(T_m-T_\infty)f^{'}+ \tag{8}$$

The negative and positive values of the variables A1 and B1, respectively, represent the heat sink/source.

Eqn. (4) can be changed by applying Eqs. (6)–(8).

$$\rho C_p\left(\nu\frac{\partial T}{\partial r}+\frac{du}{(r+d)\frac{\partial T}{\partial s}}\right)=k_\infty(1+\varepsilon\theta)\left(\frac{\partial^2 T}{\partial r^2}+\frac{1}{(r+d)\frac{\partial T}{\partial r}}\right)+\frac{\partial}{\partial r}(k_\infty(1+\varepsilon\theta))\frac{\partial T}{\partial r}-\sigma B_0^2u^2+\frac{16\sigma^*}{3k^*}\left(\frac{\partial}{\partial r}\left(T^3\frac{\partial T}{\partial r}\right)+\right. \tag{9}$$

The recommended boundary conditions for the current investigation are [3,10,15].

$$u=u_w(s),\nu=0,N=-M_r\frac{\partial u}{\partial r},T=T_w atr=0,$$

$$u\to 0,\frac{\partial u}{\partial r}\to 0,N\to 0,T\to T_\infty asr\to\infty, \tag{10}$$

Here Mr $(0\le Mr\le 1)$ denotes the micro-rotation parameter. $Mr=0$. It points out that because of the fluid's high concentration of microelements, the microelements cannot spin close to the surface of the wall.

Set out the similarity variable's definition (η) [3,10,15].

$$\eta=\sqrt{\frac{A1\upsilon e^{\frac{s}{L}}}{2L}}r, \tag{11}$$

In terms of similarity variables, now let the terms $(u,v,p,N,and\ T)$ [3,15,18]

$$u=A1e^{\frac{s}{L}}f^{'}(\eta),\nu=\frac{-d}{r+d}\sqrt{\frac{A1\upsilon e^{\frac{s}{L}}}{2L}}(f(\eta)+\eta f^{'}(\eta)),p=\rho A_1^2e^{\frac{2s}{L}}P(\eta),N=A1\sqrt{\frac{A1\upsilon e^{\frac{s}{L}}}{2L}e^{\frac{s}{L}}}g(\eta),T=T_\infty(1+(\theta_w-1)\theta(\eta)),\theta_w=T_w/T_\infty, \tag{12}$$

Temperature ratio parameter, temperature, pressure, micro-rotation and dimensionless velocity are represented here by $w,\theta(\eta),P(\eta),g(\eta),$ and$F^{'}(\eta)$ respectively.

Eqn. (1) is routinely satisfied by similarity renovations, and Eqns. (2)–(4) and (9) becomes

$$\frac{dP}{d\eta}=\frac{1}{(a_1+\eta)}\left(\frac{df}{d\eta}\right)^2, \tag{13}$$

$$\frac{a_1\eta}{(a_1+\eta)}\frac{dP}{d\eta}+\frac{4a_1}{a_1+\eta}P=(1+\alpha_1)\left(\frac{d^3f}{d\eta^3}+\frac{1}{a_1+\eta}\frac{d^2f}{d\eta^2}-\frac{1}{a_1+\eta^2}\frac{df}{d\eta}\right)-\frac{2a+\eta}{(a_1+\eta)^2}\eta\left(\frac{df}{d\eta}\right)^2+\frac{a_1}{(a_1+\eta)}f\frac{d^2f}{d\eta^2}+\frac{a_1}{(a_1+\eta)^2}f\frac{df}{d\eta}$$
$$-\alpha_1\frac{dg}{d\eta}-M\frac{df}{d\eta}+\lambda\theta, \tag{14}$$

$$\left(1+\frac{\alpha_1}{2}\right)\left(\frac{d^2g}{d\eta^2}+\frac{1}{(a+\eta)}\frac{dg}{d\eta}\right)+\frac{a_1}{(a+\eta)}\left(f\frac{dg}{d\eta}-\frac{df}{d\eta}g\right) \tag{15}$$

$$(1+\varepsilon\theta)\left(\frac{d^2\theta}{d\eta^2}+\frac{1}{(a_1+\eta)}\frac{d\theta}{d\eta}+\mathrm{A1}\frac{df}{d\eta}+\mathrm{B1}\theta\right)+\varepsilon\left(\frac{d\theta}{d\eta}\right)^2+\frac{a_1}{a_1+\eta}Prf\frac{d\theta}{dn}-PrMEc\left(\frac{df}{d\eta}\right)^2+\mathrm{Nr}\left((1+(\theta_w-1)\theta^3\left(\frac{d^2\theta}{d\eta^2}+\frac{1}{(a_1+\eta)}\frac{d\theta}{d\eta}\right)+3\right. \tag{16}$$

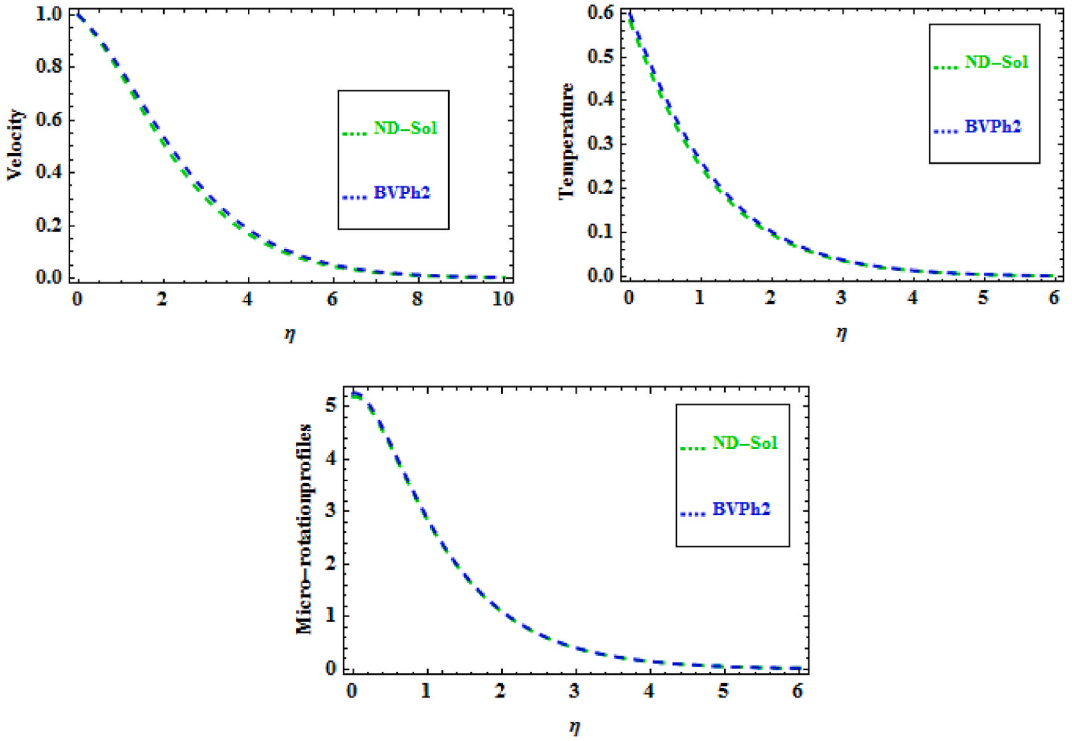

Fig. 2. Comparison of ND-Solve, and BVPh2.

Table 1
Validation of the present work by comparison with the published work.

a_1	Present work	Published work [3]
0.5	1.52072	1.52075
1.0	1.45784	1.45782
1.5	1.42461	1.42466
2.0	1.41396	1.41392
2.5	1.30863	1.30860
3.0	1.30557	1.30558
4.0	1.39922	1.39925

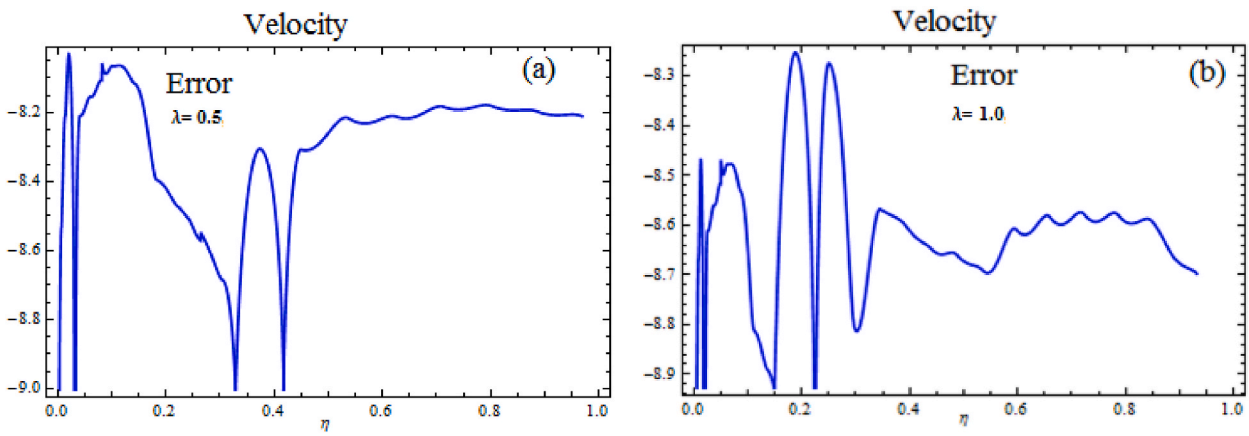

Fig. 3. (A, b). Error analysis for (a) $\lambda = 0.5$ and (b) $\lambda = 1.0$.

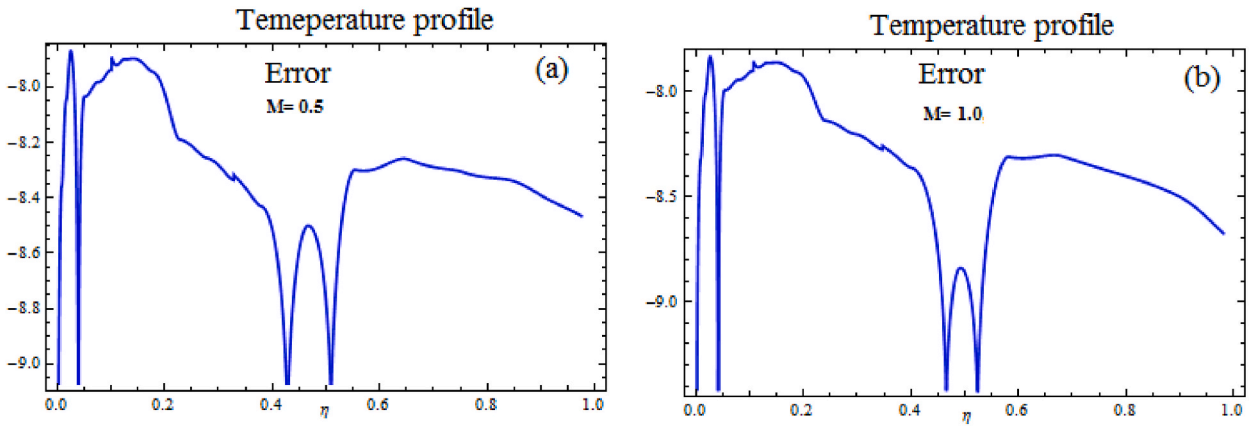

Fig. 4. (A, b). Error analysis for (a) $M = 0.5$ and (b) $M = 1.0$.

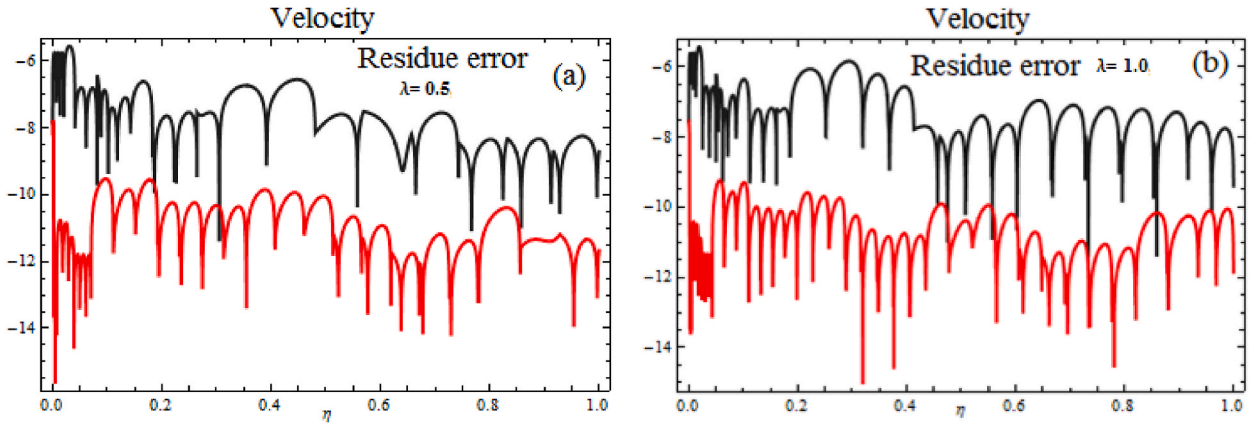

Fig. 5. (A, b). Residue error for (a) $\lambda = 0.5$ and (b) $\lambda = 1.0$..

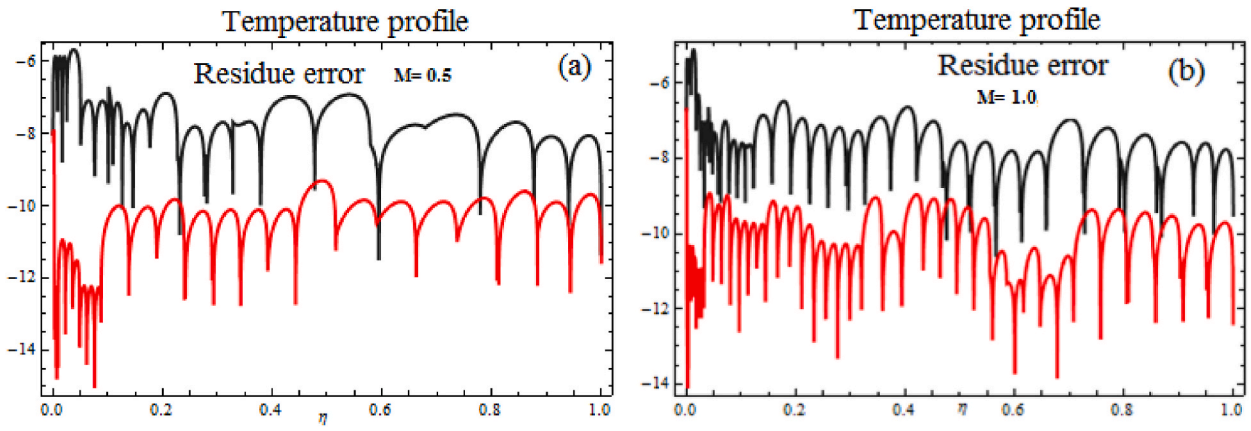

Fig. 6. (A, b). Residue error for (a) $M = 0.5$ and (b) $M = 1.0$.

Here, $Pr = \frac{\mu C_p}{k}$ is Prandtl number, $\lambda = \frac{g\beta_T(T-T_\infty)2L}{(u_w)^2\upsilon}$ is Eckert number, $\mathrm{Nr} = \frac{16\sigma^* T_\infty^3}{3k_\infty k^*}$ is nonlinear radiation factor, $a_1 = d\sqrt{\frac{A1e^{s/L}}{2\upsilon L}}$ is curvature factor and $M = \frac{\sigma B_0^2}{A1\rho}$ is the convection factor.

The modified boundary conditions include

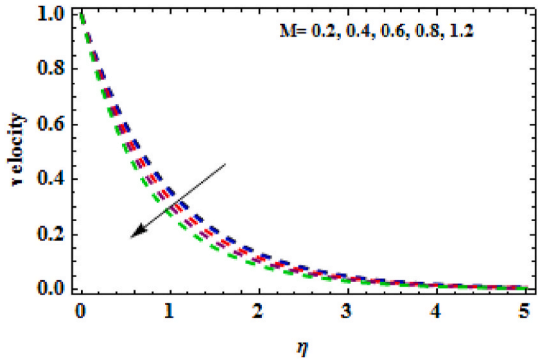

Fig. 7. Inspiration of M via velocity.

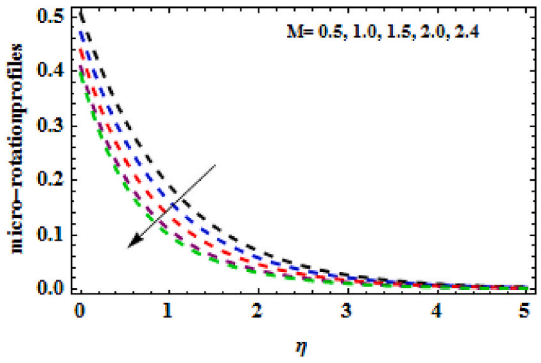

Fig. 8. Inspiration of M via microrotation.

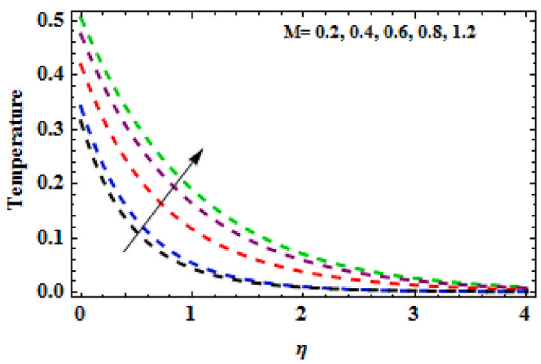

Fig. 9. Inspiration of M via temperature.

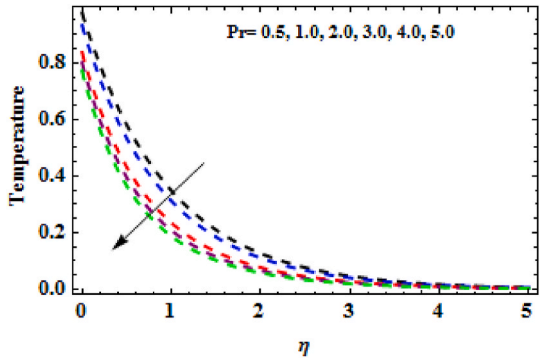

Fig. 10. Inspiration of M via temperature.

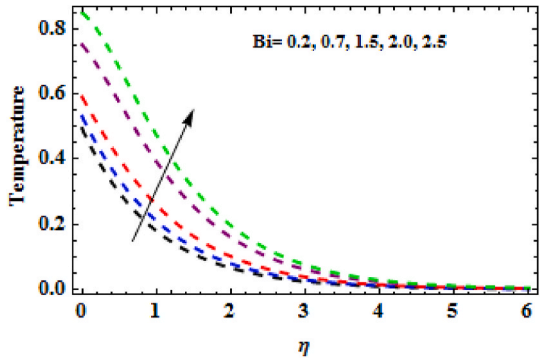

Fig. 11. Inspiration of *Bi* via temperature.

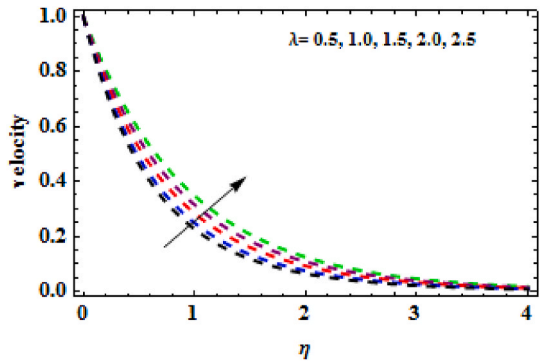

Fig. 12. Inspiration of λ via temperature.

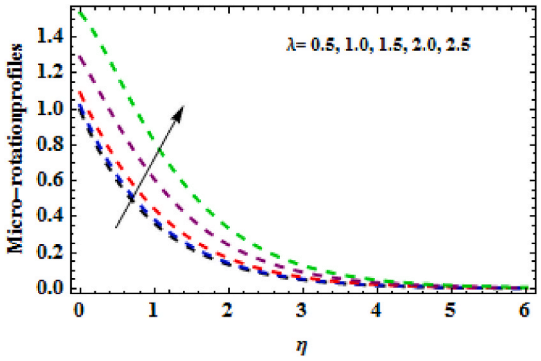

Fig. 13. Inspiration of λ via microrotation.

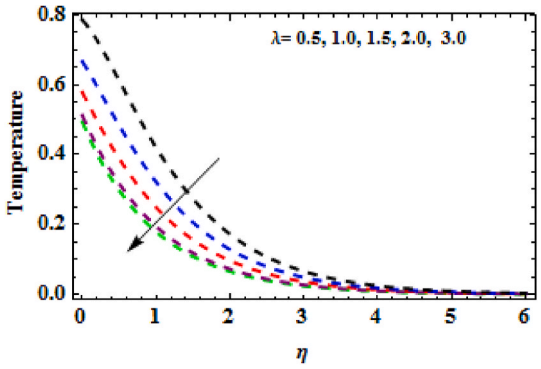

Fig. 14. Inspiration of λ via temperature.

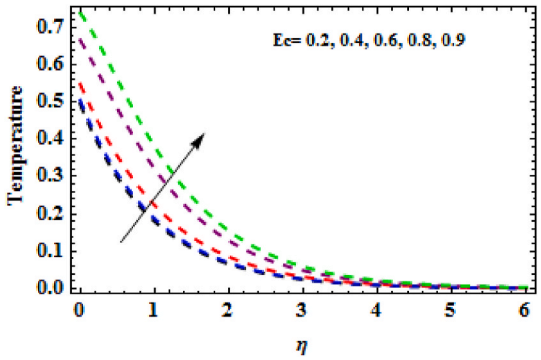

Fig. 15. Influence of *Ec* via temperature.

$$f(0)=0, f'(0)=1, g=-Mrf''(0), \theta'^{(0)}=-Bi(1-\theta(0))$$

$$, f'(\infty)\to 0, f''(\infty)\to 0, g(\infty)\to 0, \theta(\infty)\to 0. \tag{17}$$

After eradicating the pressure term (13) and (14), we obtain

$$(1+\alpha_1)\left(\frac{d^4f}{d\eta^4}+\frac{2}{(a_1+\eta)}\frac{d^3f}{d\eta^3}-\frac{1}{(a_1+\eta)^2}\frac{d^2f}{d\eta^2}+\frac{1}{(a_1+\eta)^3}\frac{df}{d\eta}\right)-\frac{\alpha_1}{4a}\left(\frac{dg}{d\eta}+(a+\eta)\frac{d^2g}{d\eta^2}\right)+\frac{a_1}{(a_1+\eta)}\left(\left(f\frac{d^3f}{d\eta^3}+\frac{1}{(a_1+\eta)}f\frac{d^2f}{d\eta^2}\right.\right.$$
$$\left.\left.-\frac{1}{(a_1+\eta)^2}f\frac{df}{d\eta}\right)-3\frac{df}{d\eta}\left(\frac{1}{(a_1+\eta)}\frac{df}{d\eta}+\frac{d^2f}{d\eta^2}\right)\right)+\frac{\alpha_1}{(a_1+\eta)}\left(\lambda\frac{d\theta}{d\eta}-M\frac{d^2f}{d\eta^2}\right)=0 \tag{18}$$

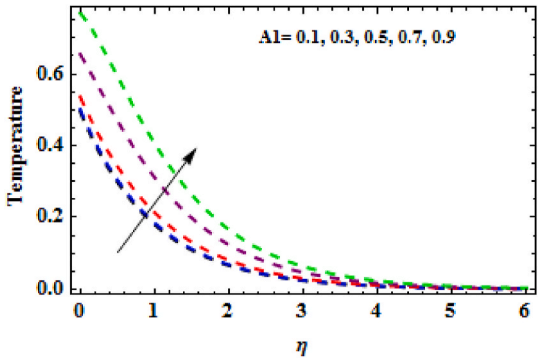

Fig. 16. Inspiration of $A1$ via temperature.

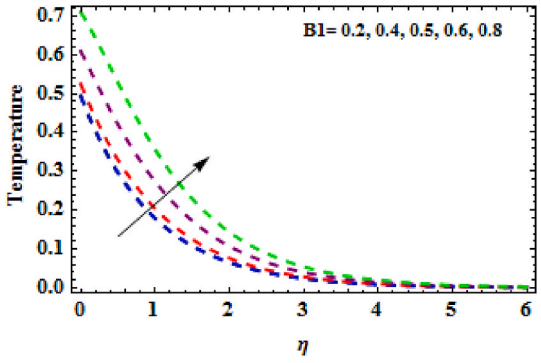

Fig. 17. Influence of $B1$ via temperature.

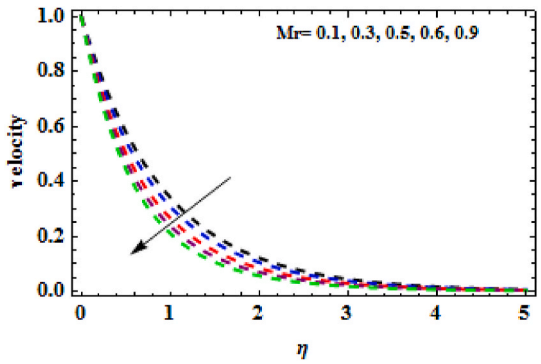

Fig. 18. Inspiration of Mr via velocity.

In engineering, manufacturing and industrial processes, the dual stress coefficient, local Nusselt number, and friction factor are essential applications of the current problem. These are identified as

$$C_F = \frac{\tau_w}{\frac{1}{2}\rho(u_w)^2}, C_s = \frac{M_w}{\mu j u_w}, Nu = \frac{s j_w}{k_\infty (T_w - T_\infty)}, \tag{19}$$

The surface heat flow, couple stress, and shear stress are shown here as

$$\tau_s = ((\mu + \kappa)\left(\frac{\partial u}{\partial r} - \frac{u}{r+d}\right) + \kappa N\Big)_{r=0}, M_w = (\mu + \frac{\kappa}{2})j\left(\frac{\partial N}{\partial r}\right)_{r=0} \text{and} q_s = -k(T)\left(\frac{\partial T}{\partial r}\right)_{r=0} + q_f.$$

Eqn. (12) transforms Eqn. (19) into

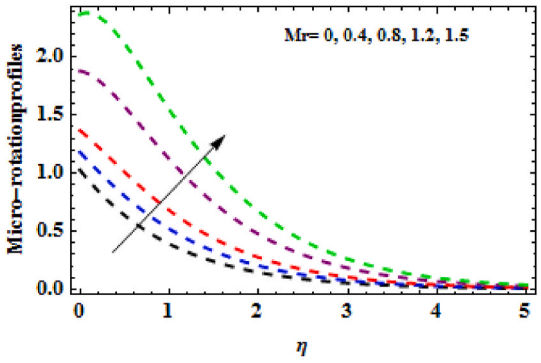

Fig. 19. Inspiration of *Mr* via microrotation.

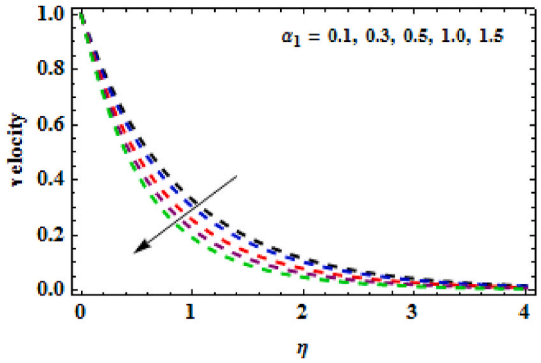

Fig. 20. Inspiration of α_1 via velocity.

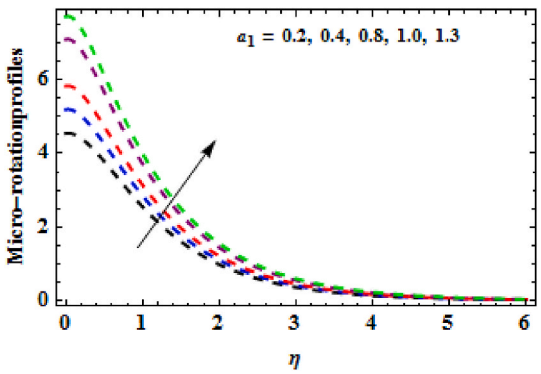

Fig. 21. Influence of α_1 via microrotation.

$$Re_s^{1/2} C_F = 2((1+\alpha_1)\left(\frac{d^2 f}{d\eta^2} - \frac{1}{\alpha_1}\frac{df}{d\eta}\right)_{\eta=0} - \alpha_1 M_r \left(\frac{d^2 f}{d\eta^2}\right)_{\eta=0}),$$

$$C_s = \left(1+\frac{\alpha_1}{2}\right)\left(\frac{dg}{d\eta}\right)_{\eta=0}, Re_s^{-1/2} Nu = -\left(1+N_r\theta_w^3\right)\left(\frac{d\theta}{d\eta}\right)_{\eta=0}, \tag{20}$$

in which $Re_s = \frac{u_w(s)L}{\upsilon}$ is localized Reynolds number.

3. Numerical procedure and validation

The scheme of nonlinear Eqs. (15), (16) and (18) corresponding to conditions (18) are elucidated numerically through ND-Solve

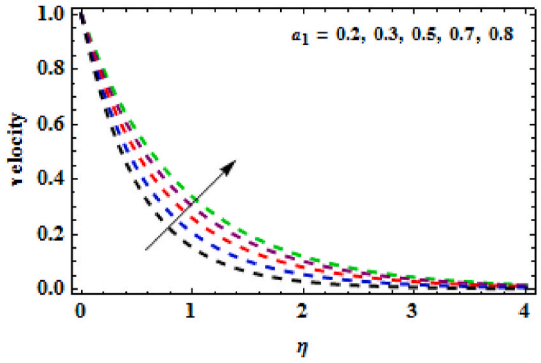

Fig. 22. Influence of a_1 via velocity.

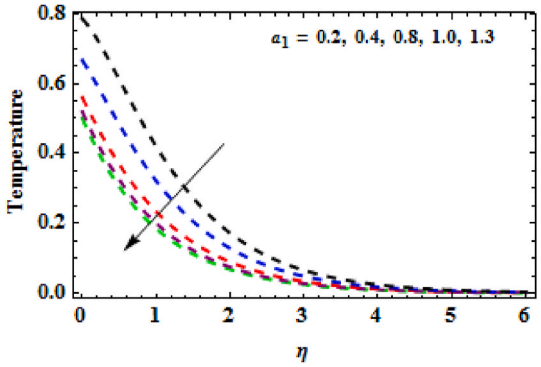

Fig. 23. Influence of a_1 via temperature.

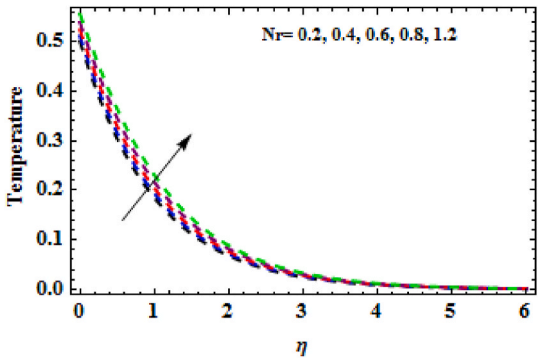

Fig. 24. Influence of *Nr* via temperature.

approach. For the existing work, precision 10^{-4} is established. To confirm the numerical solution, BVPh2 is also applied and outstanding correspondence is established as demonstrated in Fig. 2.

4. Validation analysis

To certify the precision of the above mathematical model, the present study is validated with the previous [3] for the several values of a_1 and outstanding settlement is established as revealed in Table 1. In Table 1, the results of Okechi et al. [3] are used to validate the present friction factor results with different values of a_1. Because of their consequences, we come to a strong agreement. The increasing values of reducing the friction factor may be seen from there.

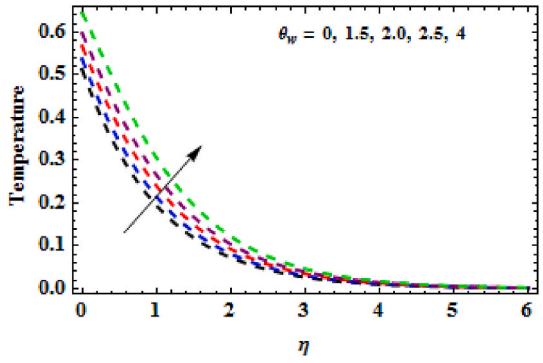

Fig. 25. Influence of θ_w via temperature.

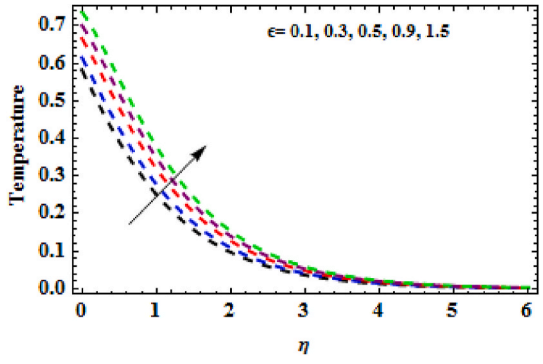

Fig. 26. Influence of ϵ via temperature.

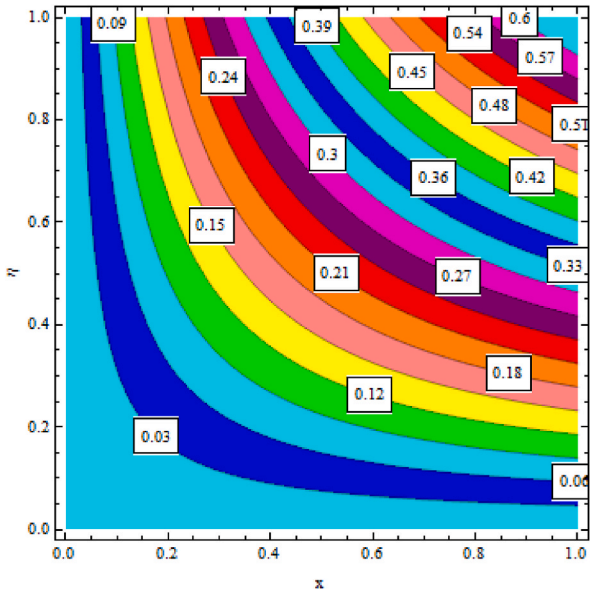

Fig. 27. Streamlines for $\lambda = 0.5$..

5. Error explanation

The RK4 technique produces results for the majority of mathematical problems that are generally reliable. The results rely on machine testing and error estimations, thus significant mistakes are quite unlikely. It is usually beneficial to examine the findings

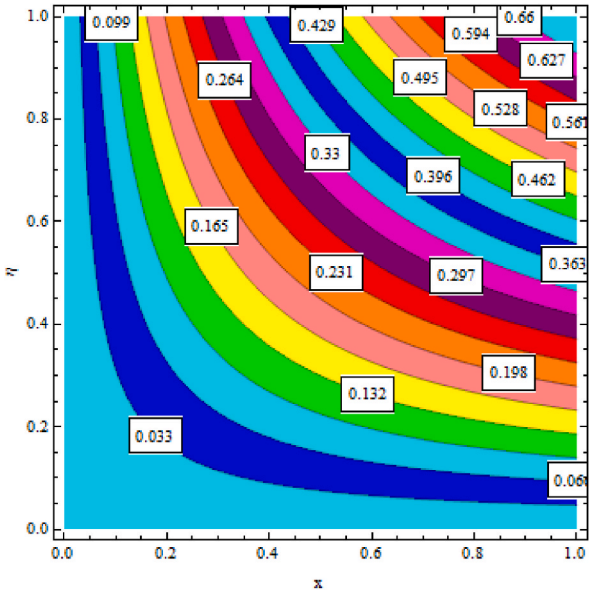

Fig. 28. Streamlines for $\lambda = 1.0$..

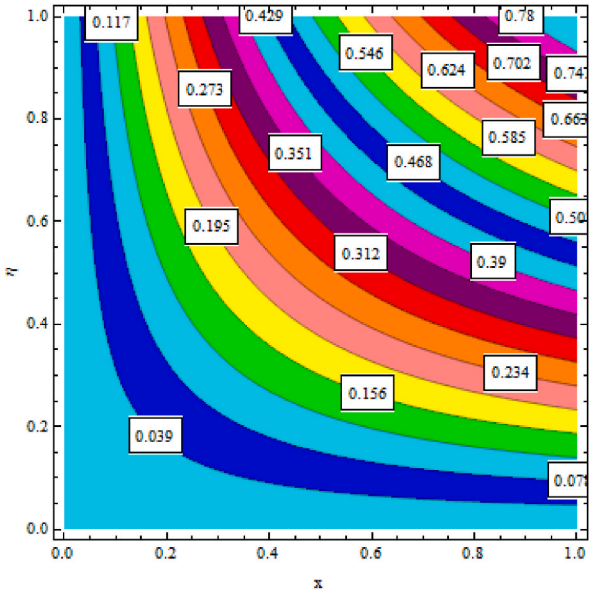

Fig. 29. Streamlines for $\lambda = 1.5$..

utilizing a solution that was developed with operational precision greater than the Normal Machine Precision (NMP). The problem's solution is computed using the RK4 technique with NWP, and the resulting error is computed with WP-22 using the same approach. It is better to assess errors with a scale based on logarithmic functions since they are often rather minor. The erroneous consequences produced for the different physical variables used in the method are displayed via graphs.

Before making any physical projections, we first computed an evaluation of errors to ensure that the procedure is trustworthy. We created Fig. 3(a and b)–6 (a, b) to examine the error analysis. For this analysis the error is fixed with 10–15. Figs. 3 and 4 show the maximum MSRE at numerous estimates. It is perceived that the error is declined with enhancing order of iterations as explored in Fig. 3 (a, b) and 4 (a, b), respectively for different values of λ and M. Similarly, the residue errors are computed in Fig. 5 (a, b) and 6 (a, b). It is significant to note that error for $\lambda = 0.5 > \lambda = 1.0$ and$M = 0.5 > M = 1.0$ (see Fig. 6).

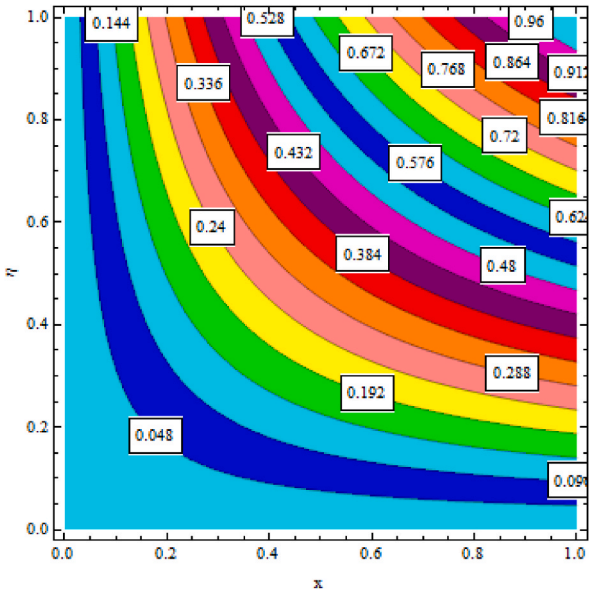

Fig. 30. Streamlines for $\lambda = 2.0$..

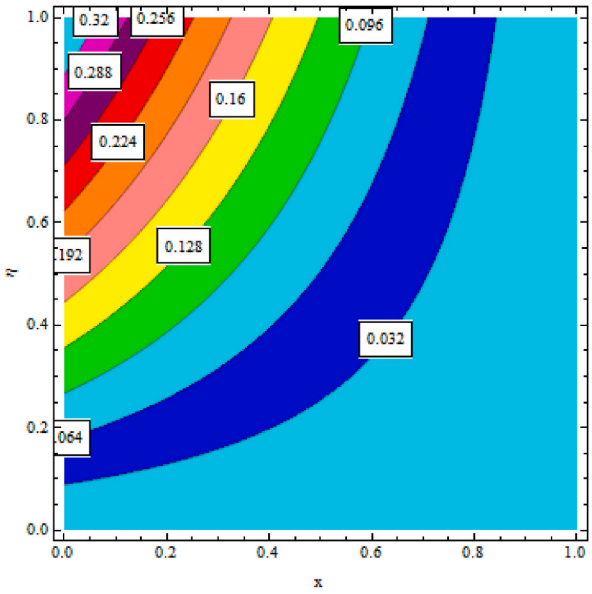

Fig. 31. Isothermal lines for $Nr = 0.2$..

6. Results and discussion

The dimensionless modelled system of ODEs given in Eqs. (13)–(17) are computed numerically by ND-Solve technique. Graphical representation is used to show how different dimensionless factors affect the flow characteristics, such as temperature, micro-rotation, and velocity. Outcomes are obtained by choosing the values of dimensionless factor as $\alpha_1 = 1.2, M = 0.3, A1 = B1 = 0.2, Pr = 5, \lambda = 0.4, \varepsilon = 0.1, \eta = 1, Ec = 1.2, Nr = 0.5, w = 1.3,$ and$Mr = 0.1$.

To determine how magnetic factor M affects the $f(\eta)$, $g(\eta)$ and $\theta(\eta)$, Figs. 7–9 are generated. With increasing magnetic parameter values, the dispersion of velocity and micro-rotation become smaller. In reality, a strong magnetic field causes a resistive force known as the Lorentz force to arise in fluid flow. Lorentz force opposes the direction of the flow. As a result, there is a significant drop in the micro-rotation and velocity outcomes. As can be seen from Fig. 9, a stronger magnetic field parameter increases fluid temperature. This results from the Lorentz force. The fluid temperature rises due to increased heat energy it produces in the flow.

In Fig. 10, the outcome of Pr on heat distribution is revealed. The temperature curves are reduced with increasing Pr values. High

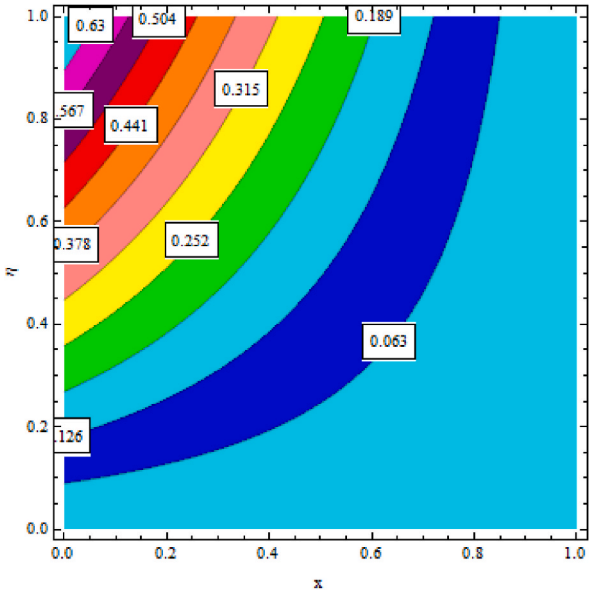

Fig. 32. Isothermal lines for $Nr = 0.4$..

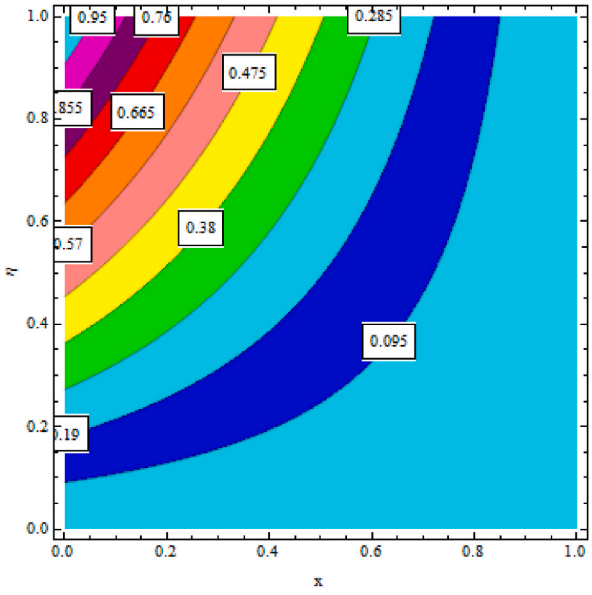

Fig. 33. Isothermal lines for $Nr = 0.9$..

conductivity results in improved layer thickness and heat function. Prandtl number is typically the momentum and thermal diffusivity ratio. Consequently, when *Pr* increases, the heat curves and associated thickness layer decreases. The outcome of the Biot number *Bi* on heat function θ (η) is discussed in Fig. 11. We can see that the temperature of the fluid is improved by elevating *Bi* values. Physically, *Bi* represents the relationship between surface convective resistance and inside conductive resistance. Therefore, when the amount of *Bi* increases, the heat curves and the BLT are enhanced.

Figs. 12–14 show how convective parameter affects the flow fields. As the values of λ increases, it is countersigned from Figs. 12 and 13 that velocity and micro-rotation increase. But the temperature curves reveal a discrete pattern (see Fig. 14). Additionally, higher values of λ lead to an increase in the viscous forces, which improves the profiles of $f'(\eta)$ and $g(\eta)$. The heat distribution function θ (η) is presented in Fig. 15 to evaluate the impact of the Eckert number. In general, *Ec* is the proportion of heat dissipation potential to advective transport. Therefore, increasing *Ec* displays to upsurge in the heat curves and BLT. Figs. 16 and 17 show how $A1$ and $B1$ have an impact on the heat function $\theta(\boldsymbol{\eta})$. It is experimented that growing $A1$ and $B1$ indications to escalation in the temperature distribution. Physically, the presence of irregular heat factors is responsible to produce temperature inside the fluid. As a result, it is found

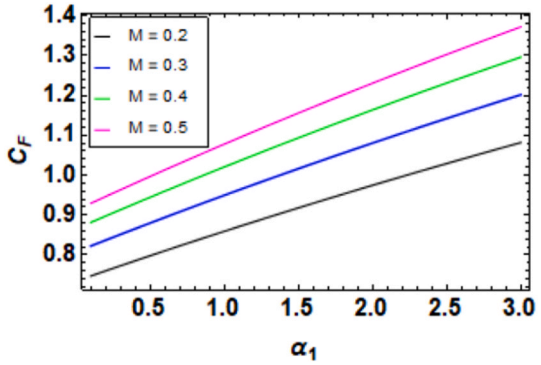

Fig. 34. Skin Friction for various values of M via α_1.

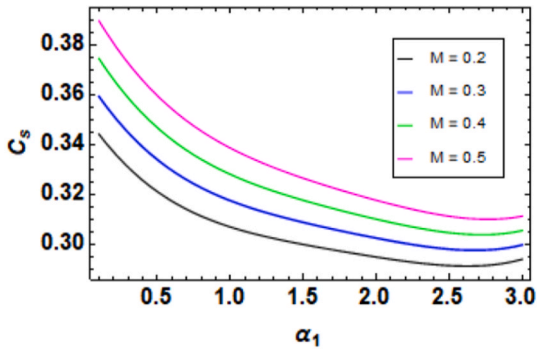

Fig. 35. Dual stress variation for different values of M.

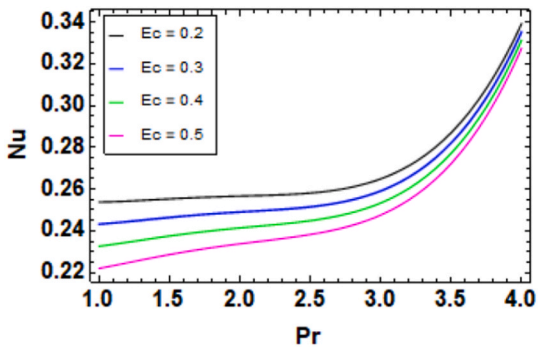

Fig. 36. Nusselt number for different values of Ec.

that the fluid temperature is improved as the values of $A1$ and $B1$ is improved.

The effects of the micro-rotation factor Mr on flow field and micro-rotation distribution are presented in Figs. 18 and 19, respectively. The scattering of micro-rotation as well as layer thickness certainly increases with increasing Mr values, although fluid velocity exhibits a contradictory development. The inspiration of α_1 (micropolar factor) on velocity and mocrorotation distribution is depicted Figs. 20 and 21, respectively. It's interesting to note that the fluid flow declines with the enhancing values of α_1. From the mathematical relation it is also countersigned that the velocity is inversely proportionate to the micro polar factor. However, the micro polar factor is directly proportional to the micro rotation profile. Figs. 22 and 23 demonstrate how the curvature parameter a_1 affects the flow and temperature fields. Noticed that temperature curve is a diminishing function of increasing a_1, whereas the situation seems to be opposite for fluid velocity. The exponential surface radius is often enriched by raising a_1 values, which increases fluid velocity and lowers temperature.

To understand the impact of temperature ratio parameter and non-linear radiation on the heat function distribution $\theta(\eta)$, Figs. 24 and 25 are illustrated. It is remarkable to footnote that, heat inside the fluid is an accelerating function of non-linear radiation factor. Typically, radiation is a heat transmission method that obtains energy from liquid grains. Consequently, it enhances the flow of heat

energy. Because of this, it is observed that the heat function improved for higher *Nr*. This is noteworthy to see that as θ_w increases in value, so does the temperature distribution. Fig. 26 illustrates the variation in heat effects function due to temperature-dependent thermal conductivity (ε). A better thermal field is most likely provided by larger ε. Stream lines for the various values of $\lambda = 0.5, 1.0,$ 1.5, and2 are given in Figs. 27–30. It is observed that the steam lines behave increasing behaviour for λ. It is observed that for larger magnitude of λ higher variation is observed for the stream lines. The isothermal lines are depicted in Figs. 31–33 for the numerous of $Nr = 0.2, 0.4,$ and 0.9. It is analysed that the isothermal inside the fluid rises with the increment values of *Nr*. Higher isothermal phenomena is investigated for the higher values of *Nr*.

The impact of magnetic factor on the skin friction and couple stress is shown in Figs. 34 and 35 respectively. It is detected that both the skin friction and the couple stress increases with increasing values of magnetic factor. Physically, magnetic field observes as a resistant force that works as a drag-force so called the Lorentz force. Such force resists the flow which declines the velocity of the fluid and enhances the skin friction and the dual stress. Similarly, the effect of *Ec* on the Nusselt number is shown in Fig. 36. It is investigated that the Nusselt number is an enhancing function of *Ec*.

7. Conclusions

The aim of this study is to investigate the properties of heat transfer on a magnetohydrodynamic free convection movement of micro polar fluid over an exponentially stretchable curved surface. The flow is non-turbulent and steady. The effects of Joule heating, varying thermal conductivity, irregular heat reservoir, and non-linear radiation are anticipated. The modelled PDEs are converted to ODEs via transformation, and the integration problems are then addressed using ND-Solve method along with bvp4c package. The key findings of the present study are.

- It is witnessed that the temperature of the fluid enhances as the Eckert number is augmented.
- It is observed that velocity is reduced and the micro rotation field is increased as the micro rotation parameter is increased.
- The velocity distributions enhances as the curvature parameter is improved. Furthermore, it analysed that the velocity distribution is a decreasing function of magnetic field and micro polar parameter.
- The distribution of temperature is improved by a rise in temperature-dependent thermal conductivity characteristic.
- Greater values of the temperature ratio, Prandtl number, and the Biot number of nonlinear radiation improve temperature distribution; however the temperature declines for higher values of *Pr* and convective factor.

Data availability

"Data will be made available on request".

CRediT authorship contribution statement

Aisha M. Alqahtani: Validation, Supervision, Formal analysis, Data curation, Conceptualization. **Zeeshan:** Writing – original draft, Resources, Investigation, Conceptualization. **Waris Khan:** Writing – review & editing, Software, Methodology, Conceptualization. **Amina:** Visualization, Resources, Data curation, Conceptualization. **Somayah Abdualziz Alhabeeb:** Writing – review & editing, Validation, Supervision, Project administration, Conceptualization. **Hamiden Abd El-Wahed Khalifa:** Writing – review & editing, Visualization, Validation, Supervision, Formal analysis, Conceptualization.

Declaration of competing interest

No conflict of interest exist about this manuscript.

Acknowledgments

Princess Nourah bint Abdulrahman University Researchers Supporting Project number (PNURSP2023R52), Princess Nourah bint Abdulrahman University, Riyadh, Saudi Arabia.

References

[1] M. Sheikholeslami, M. Hatami, D.D. Ganji, Micropolar fluid flow and heat transfer in a permeable channel using analytical method, J. Mol. Liq. 194 (2014) 30–36.
[2] A. Rehman, S. Nadeem, M.Y. Malik, Boundary layer stagnation-point flow of a third-grade fluid over an exponentially stretching sheet, Braz. J. Chem. Eng. 30 (2013) 611–618.
[3] N.F. Okechi, M. Jalil, M. S. Asghar, Flow of viscous fluid along an exponentially stretching curved surface, Results Phys. 7 (2017) 2851–2854.
[4] S.H.M. Saleh, N.M. Arifin, R. Nazar, I. Pop, Unsteady Micropolar fluid over a permeable curved stretching shrinking surface, Math. Probl Eng. 2017 (2017). Article ID 3085249.
[5] M. Naveed, Z. Abbas, N. Sajid, J. Hasnain, Dual solutions in hydromagnetic viscous fluid flow past a shrinking curved surface, Arabian J. Sci. Eng. 43 (2018) 1189–1194.
[6] K. Anantha Kumar, J.V.R. Reddy, V. Sugunamma, N. Sandeep, Simultaneous solutions for MHD flow of Williamson fluid over a curved sheet with non-uniform heat source/sink, Heat Tran. Res. 50 (2019) 581–603.

[7] K.A. Kumar, J.V.R. Reddy, V. Sugunamma, N. Sandeep, MHD flow of chemically reacting Williamson fluid over a curved/flat surface with variable heat source/sink, Int. J. Fluid Mech. Res. 46 (5) (2019) 407–425, https://doi.org/10.1615/InterJFluidMechRes.2018025940.
[8] A. Nadeem, K. U Rehman, W. Shatanawi, M.Y. Malik, Numerical study of heat transfer in hybrid nanofluid flow over permeable nonlinear stretching curved surface with thermal slip, Int. Commun. Heat Mass Tran. 135 (2022), 106107.
[9] A.S. Alshomrani, T. Gul, A convective study of Al2O3-H2O and Cu-H2O nano-liquid films sprayed over a stretching cylinder with viscous dissipation, Eur. Phys. J. Plus 132 (2017), https://doi.org/10.1140/epjp/i2017-11740-1.
[10] A. Nadeem, W. Shatanawi, K. Abodayeh, Computational analysis of MHD nonlinear radiation casson hybrid nanofluid flow at vertical stretching sheet, Symmetry 14 (7) (2022) 1494.
[11] K. Anantha Kumar, B. Ramadevi, V. Sugunamma, Impact of Lorentz force on unsteady bio convective flow of Carreau fluid across a variable thickness sheet with non-Fourier heat flux model, Defect Diffusion Forum 387 (2018) 474–497.
[12] K. Anantha Kumar, V. Sugunamma, N. Sandeep, J.V.R. Reddy, Impact of Brownian motion and thermophoresis on bio convective flow of nanoliquids past a variable thickness surface with slip effects, Multidiscip. Model. Mater. Struct. 15 (2019) 103–132.
[13] A. Nadeem, K.U. Rehman, W. Shatanawi, A.A. Al-Eid, Theoretical study of non-Newtonian micropolar nanofluid flow over an exponentially stretching surface with free stream velocity, Adv. Mech. Eng. 14 (7) (2022), 16878132221107790.
[14] N. Sandeep, C. Sulochana, B.R. Kumar, Unsteady MHD radiative flow and heat transfer of a dusty nanofluid over an exponentially stretching surface, Eng. Sci. Tech., Int. J. 19 (2016) 227–240, 2016.
[15] Z. Abbas, M. Naveed, M. Sajid, Hydrodynamic slip flow of nanofluid over a curved stretching surface with heat generation and thermal radiation, J. Mol. Liq. 215 (2016) 756–762.
[16] T. Hayat, M.M. Rashidi, M. Imtiaz, A. Alsaedi, MHD convective flow due to a curved surface with thermal radiation and chemical reaction, J. Mol. Liq. 225 (2017) 482–489.
[17] A. Zeeshan, A. Majeed, R. Ellahi, Effect of magnetic dipole on viscous ferro-fluid past a stretching surface with thermal radiation, J. Mol. Liq. 215 (2016) 549–554.
[18] K Anantha Kumar, V. Sugunamma, N. Sandeep, Impact of non-linear radiation on MHD non-aligned stagnation point flow of micropolar fluid over a convective surface, J. Non-Equil. Thermodyn (2018), https://doi.org/10.1515/jnet-2018-0022.
[19] T. Hayat, S. Farooq, B. Ahmad, A. Alsaedi, Homogeneous-Heterogeneous reactions and heat source/sink effects in MHD flow of micropolar fluid with Newtonian heating in a curved channel, J. Mol. Liq. 223 (2016) 469–488.
[20] K. Mehmood, S. Hussain, M. Sagheet, Mixed convection flow with non-uniform heat source/sink in a doubly stratified magnetonanofluid, AIP Adv. 6 (2016), https://doi.org/10.1063/1.4955157.
[21] K. Gangadhar, K.R. Venkata, O.D. Makinde, B.R. Kumar, MHD flow of a Carreau fluid past a stretching cylinder with Cattaneo-Christov heat flux using spectral relaxation method, Defect Diffusion Forum 387 (2018) 91–105.
[22] T.S. Kumar, B.R. Kumar, O.D. Makinde, A.G. Vijaya Kumar, Magneto-convective heat transfer in micropolar nanofluid over a stretching sheet with non-uniform heat source/sink, Defect Diffusion Forum 387 (2018) 78–90.
[23] A. Nadeem, W. Shatanawi, Heat and mass transfer of micropolar-casson nanofluid over vertical variable stretching riga sheet, Energies 15 (14) (2022) 4945.
[24] M. Ramzan, M. Farooq, T. Hayat, J.D. Chung, Radiative and Joule heating effects in the MHD flow of a micropolar fluid with partial slip and convective boundary condition, J. Mol. Liq. 221 (2016) 394–400.
[25] A.A. Khan, R. Rafaqat, Effects of radiation and MHD on compressible Jeffrey fluid with peristalsis, J. Therm. Anal. Calorim. 143 (2021) 2775–2787.
[26] M.S. Abel, N. Mahesha, Heat transfer in MHD viscoelastic fluid flow over a stretching sheet with variable thermal conductivity, non-uniform heat source and radiation, Appl. Math. Model. 32 (2008) 1965–1983.
[27] A.A. Khan, R. Batool, N. Kousar, Examining the behavior of MHD micropolar fluid over curved stretching surface based on the modified Fourier law, Sci. Iran. 28 (1) (2021) 223–230.
[28] M.Y. Malik, M. Bibi, F. Khan, T. Salahuddin, Numerical Solution of Williamson Fluid Flow Past a Stretching Cylinder and Heat Transfer with Variable Thermal Conductivity and Heat Generation/absorption, AIP Adv, vol. 6, 2016. Article ID: 035101.
[29] K. Anantha Kumar, J.V.R. Reddy, V. Sugunamma, N. Sandeep, Impact of cross diffusion on MHD viscoelastic fluid flow past a melting surface with exponential heat source, Multidiscip. Model. Mater. Struct. (2018), https://doi.org/10.1108/MMMS-12-2017-0151.
[30] D. Srinivasacharya, P. Jagadeeshwar, Effect of variable properties on the flow over an exponentially stretching sheet with convective thermal conditions, Modell., Meas. Control, B 87 (2018) 7–14.
[31] M.A.S. Metwally, A. Khalid, A.A. Khan, K. Iskakova, M.R. Gorji, M. Ehab, Radiation consequences on Sutterby fluid over a curved surface, J. Eng. Thermophys. 31 (2) (2022) 315–327.
[32] O.D. Makinde, I.L. Animasaun, Thermophoresis and Brownian motion effects on MHD bioconvection of nanofluid with nonlinear thermal radiation and quartic chemical reaction past an upper horizontal surface of a paraboloid of revolution, J. Mol. Liq. 221 (2016) 733–743.
[33] O.D. Makinde, N. Sandeep, I.L. Animasaun, M.S. Tshehla, Numerical exploration of Cattaneo- Christov heat flux and mass transfer in magnetohydrodynamic flow over various geometries, Defect Diffusion Forum 374 (2017) 67–82.